Fermi National Accelerator Laboratory

FERMILAB-Pub-92/203

Antiproton-Proton Elastic Scattering at $\sqrt{s}$ = 1020 GeV

The E710 Collaboration

N.A. Amos(3), C.Avila(3), W.F. Baker(3), M. Bertani(1), M.M. Block(7), D. Dimitroyannis(7), D.P. Eartly(3), R.W. Ellsworth(5), G. Giacomelli(1), B. Gomez(3,4), J.A. Goodman(6), C.M. Guss(7), A.J. Lennox(3), M.R. Mondardini(2), J.P. Negret(3,4), J. Orear(2), S.M. Pruss(3), R. Rubinstein(3), S.Sadr(7), J.C. Sanabria(3), S. Shukla(3), M. Spagnoli(1), I. Veronesi(1), and S. Zucchelli(1)

(1) Universita' di Bologna and Istituto Nazionale di Fisica Nucleare, Bologna, Italy
(2) Cornell University, Ithaca, New York 14853
(3) Fermi National Accelerator Laboratory, Batavia, Illinois 60510
(4) Universidad del Los Andes, Bogota, Colombia
(5) George Mason University, Fairfax, Virginia 22030
(6) University of Maryland, College Park, Maryland 20742
(7) Northwestern University, Evanston, Illinois 60201

August 1992

Submitted to *Il Nuovo Cimento A*

Operated by Universities Research Association Inc. under Contract No. DE-AC02-76CHO3000 with the United States Department of Energy

Disclaimer

ANTIPROTON-PROTON ELASTIC SCATTERING AT $\sqrt{s} = 1020\,GeV$

N.A. Amos[3], C. Avila[3a], W.F. Baker[3], M. Bertani [1b], M. M. Block[7], D. Dimitroyannis[7], D.P. Eartly[3], R.W. Ellsworth[5], G. Giacomelli[1], B. Gomez[3,4], J.A. Goodman[6], C.M. Guss[7d], A.J. Lennox [3], M.R. Mondardini[2e], J.P. Negret[3,4], J. Orear[2], S.M. Pruss[3], R. Rubinstein[3], S. Sadr[7], J. C. Sanabria[3], S. Shukla[3], M. Spagnoli[1], I. Veronesi[1] and S. Zucchelli[1]

(The E710 collaboration)

(1) Universita' di Bologna and Istituto Nazionale di Fisica Nucleare,Bologna, Italy
(2) Cornell University, Ithaca, New York 14853
(3) Fermi National Accelerator Laboratory, Batavia, Illinois 60510
(4) Universidad del Los Andes, Bogota, Colombia
(5) George Mason University, Fairfax, Virginia 22030
(6) University of Maryland, College Park, Maryland 20742
(7) Northwestern University, Evanston, Illinois 60201

ABSTRACT

The antiproton-proton small angle elastic scattering distribution was measured at $\sqrt{s} = 1020\,GeV$ at the Fermilab Tevatron Collider.
A fit to the nuclear scattering distribution in the range $0.065 \leq |\,t\,| \leq 0.21\,(GeV/c)^2$ gives $b = (16.2 \pm 0.5 \pm 0.5)\,(GeV/c)^{-2}$ for the logarithmic slope parameter. Using the optical theorem and the luminosity from Collider parameters, we obtain $\sigma_{tot}(1+\rho^2)^{1/2} = (61.7 \pm 3.7 \pm 4.4)\,mb$.

PAC 13.85.DZ
Submitted to Il Nuovo Cimento A
Bologna, 9/July/1992

1. Introduction

High energy $p\bar{p}$ elastic scattering angular distributions in the t range $0.01 \leq |t| \leq 0.70\,(GeV/c)^2$ have been measured in a number of experiments [1-8]. The distribution is consistent at $\sqrt{s} = 1.8\,TeV$ with a simple exponential form, while at lower energies the data were usually fit by two exponentials, one in the range $|t| \leq 0.15\ (GeV/c)^2$, and the other for larger $|t|$. The corresponding logarithmic slope parameters were found to be different by about $2\,(GeV/c)^{-2}$, with the larger b values at smaller $|t|$. Some experiments found satisfactory fits with a quadratic exponential form. In this letter we report on new data on $p\bar{p}$ elastic scattering obtained at the Fermilab Tevatron Collider at $\sqrt{s} = 1020\,GeV$, in the t range $0.065 \leq |t| \leq 0.21\,(GeV/c)^2$. Because of the limited t range it was not possible to test whether two exponentials were required to fit the t-distribution at this energy.

2. Data

The data were collected in 1989 during a dedicated run of the Collider. Fig. 1 shows a schematic layout of the apparatus, whose details are described elsewhere [6]. For these data, the inner "Roman Pots", located $25\,m$ from the interaction point $E0$, were used. A four wire drift chamber and three scintillation counters, two used for triggering and the other for calibration purposes, were housed in each pot.

An elastic event requires a hit in the upper (lower) detector in the left side inner pot in coincidence with a hit in the lower (upper) detector of the right side inner pot. Such a combination is referred to as a conjugate pair of pots. Due to the Tevatron injection magnets located between the interaction point $E0$ and the inner pots, part of the acceptance region of the combination *up left – down right* was obscured, so only the combination *down left – up right* was used in the analysis. In addition the non-conjugate pairs, i.e. up (down) left in coincidence with up (down) right, were also recorded for background subtraction purposes.

The trigger was a 2-fold coincidence of scintillation counters in the two inner pots used in the analysis. A total of 864890 triggers was recorded. In order to obtain the final sample of elastic events several cuts were applied:

a) The timing of signals from the scintillation trigger counters in each pot must lie in a narrow window corresponding to the time of flight of events originating in the interaction region. Events outside this window were rejected.

b) The pulse height of the signals from the trigger counters must be above a given threshold in order to reduce triggering caused by photomultiplier noise; the threshold was well below the pulse height of a minimum ionizing particle.

c) Events were rejected if there was a hit in any of the scintillation counters in the vicinity of the interaction region which were used for detecting inelastic events, or if there was a hit in the scintillation counters of the other two pots.

d) At least two out of three wires in each chamber were required to be hit, with the vertical coordinates within $500\,\mu m$ of each other. The overall efficiency for recording elastic events was obtained by measuring individual wires efficiencies; it was typically about 95%.

A fiducial region was defined in the left detector, both vertically and horizontally, as being the largest area, centered horizontally around the beam, not shadowed by the injection magnets. The left detector was chosen because the two conjugate pots were not symmetrically positioned vertically around the beam axis, with the left pot being further away from the beam axis than the right one. As a consequence, given the beam sizes and angular divergences, the vertical acceptance correction due to incomplete coverage in the right pot is small if the fiducial region is chosen in the left pot. A cut in the horizontal coordinate of $\pm 6\,mm$ around the beam center at the left detector was applied in order to ensure that the acceptance used was not affected by the injection magnets. Given the beam characteristics at this energy (obtained by scaling from those obtained at $\sqrt{s} = 1.8\,TeV$), the region defined above was such that horizontally the elastic distribution was completely contained in the conjugate pot, thus avoiding a horizontal acceptance correction.

After all of the cuts we were left with 8144 candidates, about 6600 of which were in the elastic event region around the diagonal of the distribution (shown in Fig. 2a) that shows the correlation between the y (vertical) coordinates in the two chambers. The drift chamber horizontal coordinate readout (based on charge division) is known with substantially less accuracy than the vertical readout (based on drift time); we therefore integrated over the horizontal (x) coordinate and used only the variation in the vertical coordinate to obtain $d\sigma/dt$.

Three runs were taken at different pot positions, and the left drift chamber's closest approach to the beam center varied from 10 to $12\,mm$. In Fig. 2a we can see a substantial background in the elastic distributions at the smallest distances from the circulating beams. The background is mainly due to the beam halo.

To estimate backgrounds, the "non-conjugate" pair of pots was used. The background on the right hand side (due to proton beam halo) is almost independent of the background on the left hand side (due to the antiproton beam halo). Therefore the background in each detector of the elastic combination was obtained from events where there was a hit in the non-conjugate pot on the other side of the interaction region; the same cuts were applied as for the elastic candidates. The two distributions so obained were then combined to produce the background distribution shown in Fig. 2b. Extensive studies showed that the shape of the background distribution in Fig. 2b is identical to that of the background in Fig. 2a, as expected. The background obtained in this way was then normalised to that in the conjugate pair distribution outside the elastic region and subtracted bin by bin.

The ratio of background to signal in the first few millimeters from the beam of the chamber was about 17% in the first run, when the pots were further away from the beam, and about 50% in the following runs; the background became negligible after the first few millimeters.

3. Elastic angular distribution

We used the form $dN/dt = A\,exp(bt)$ for the elastic distribution where N is the number of events, and derived the logarithmic slope parameter b. As mentioned earlier, since we integrated over the x coordinate, we actually used dN/dy, where each y bin covered a range of t. The overall t range for the data was $0.065 \leq |\, t \,| \leq 0.21\,(GeV/c)^2$. In order to use the y range covered by all the three runs which had different pot positions, the lower y limit was determined by the highest of the three minimum y limits reached. The upper

y value was set by the fiducial region not shadowed by the injection magnets in the left pot, in the run where the pots where furthest away from the beam axis. Our result was $b = 16.2 \pm 0.5 (GeV/c)^{-2}$, where the error is statistical only. Fig. 3 shows the elastic distribution for one run.

Systematic uncertainties arise mainly from the background subtraction procedure, from the incomplete knowledge of the vertical beam position with respect to the detectors, from the uncertainty in the position of the interaction region along the beam axis, and from uncertainties in pot positions. The contribution of the background subtraction decreases as the lower y limit of the fit is increased, since the background distribution is very sharply peaked at low y. The value of b obtained with fits performed on the data after background subtraction does not change, to within the statistical errors, when the lowest y limit in the fit is changed from 12.7 to 14.5 mm. As a further check of the background subtraction procedure we fit the elastic distribution before subtraction of the background, excluding the 4 mm of the chamber closest to the beam. The slope obtained is in agreement with the value obtained after background subtraction when the first 4 mm is included; this is an indication that the background subtraction procedure is adequate.

The location along the beam axis of the interaction point was determined by timing in the inelastic scintillation counters on either side of $E0$. The position of the interaction point at $\sqrt{s} = 1020\, GeV$ was found to be the same as that for $\sqrt{s} = 1.8\, TeV$.

The overall systematic uncertainty arising from the causes listed above is estimated to be $\pm 0.5\, (GeV/c)^{-2}$. Our final b value is

$$b = 16.2 \pm 0.5 \pm 0.5\, (GeV/c)^{-2}$$

where the first error is statistical and the second is systematic. Combining them quadratically we obtain $b = 16.2 \pm 0.7\, (GeV/c)^{-2}$. This result is shown with previous data [1-8] in Fig. 4.

4. Total cross section

The total cross section may be determined by extrapolating the $p\bar{p}$ nuclear elastic scattering differential rate at small values of $|t|$ to $t = 0$. Using the optical theorem, one has

$$\left(\frac{dN}{dt}\right)_{t=0} = L \left(\frac{d\sigma}{dt}\right)_{t=0} = L\, \frac{(1+\rho^2)\sigma_{tot}^2}{16\pi\, (\hbar c)^2} \tag{1}$$

where dN/dt is the differential number of events observed for an integrated luminosity L and $(dN/dt)_{t=0}$ is its value at $t = 0$, obtained by extrapolation of the elastic distribution.

Since we are integrating over the horizontal coordinate this formula is modified in the following way

$$\sigma_{tot}^2\, (1+\rho^2) = \frac{16\pi^2\, (\hbar c)^2\, l^2\, \frac{dN}{dy}|_{y=o}}{p^2\, \eta(x_1,\, x_2)\, L} \tag{2}$$

where l is the distance from the interaction point to the detector, p is the beam momentum and

$$\eta(x_1,\ x_2) = \int_{x_1}^{x_2} exp(-bp^2\ x^2\ /l^2)\ dx$$

x_1 and x_2 are the fiducial boundaries with respect to the horizontal beam center x_0 (found by fitting the x coordinate distribution of the elastic events by a gaussian distribution). In this formula the following approximation, valid in the forward region, was used :

$$\frac{d\sigma}{dt} = \frac{\pi}{p^2}\ \frac{l^2}{L}\ \frac{d^2N}{dx\ dy} \tag{3}$$

In order to evaluate the total cross section, elastic events were used only inside the fiducial region that we have defined above.

As already mentioned the information on the x coordinate was not used in the above analysis. But to calculate the integral over x that appears in the evaluation of the total cross section a knowledge of the x calibration is necessary. The same procedure as for the calibration of the vertical coordinate was used.

Due to degradation in the drift chamber wire performances and insufficient statistical accuracy, it was only possible to obtain the horizontal calibration for one run, and only this run was used for the determination of the total cross section. We obtain : $\sigma_{tot}(1+\rho^2)^{1/2} = (61.7 \pm 3.7)\,mb$, where the error is statistical only. The systematic error is dominated by the $\pm 15\%$ uncertainty in the luminosity obtained from Collider parameters. The error introduced in the determination of the total cross section by the uncertainty of the x - calibration, including effects of possible non - linearity, was computed to be less than 1%. The final result is

$$\sigma_{tot}(1+\rho^2)^{1/2} = (61.7 \pm 3.7 \pm 4.4)\,mb$$

where the first error is statistical and the second systematic. Using the value $\rho = 0.140$[9] we obtain: $\sigma_{tot} = (61.1 \pm 5.7)\,mb$, where the error combines quadratically the statistical and systematic uncertainties. This is shown in Fig. 5 together with previous data. [8,10–14]

5. Conclusions

We have obtained for antiproton-proton scattering at $\sqrt{s}$ = *1020 GeV* an elastic logarithmic slope $b = (16.2 \pm 0.7))\,(GeV/c)^2$ in the t range $0.065 \leq |t| \leq 0.21\ (\mathrm{GeV/c})^2$ and $\sigma_{tot} = (61.1 \pm 5.7)\,mb$. The measured values of b and σ_{tot}, plotted in Fig. 4 and Fig. 5 as functions of s, lie on smooth curves which increase with increasing *c.m.* energy.

Acknowledgments.

We wish to thanks the Fermilab Accelerator Division staff for making these measurements possible. We gratefully acknowledge the financial support from the US Department of Energy, the US National Science Foundation, the Italian Ministero Pubblica Istruzione and the North Atlantic Treaty Organization.

References.

(a) Present address : Department of Physics, University of Massachusetts, Amherst, Massachusetts 01003.
(b) Present address : Dipartimento di Fisica dell'Universita' di Ferrara and INFN, Ferrara, Italy.
(c) Present address : Department of Physics, Northwestern University, Evanston, Illinois 60201.
(d) Present address : Cornell University, Ithaca, New York 14853.
(e) Present address : CERN, CH 1211, Geneva 23, Switzerland.

[1] D.S. Ayres *et al.* Phys. Rev. D 15 (1977) 3105.
[2] L.A. Fajardo *et al.* Phys. Rev. D 24 (1981) 46.
[3] M. Ambrosio *et al.* Phys. Lett. B 115 (1982) 495.
[4] M. Bozzo *et al.* Phys. Rev. Lett. B 147 (1984) 385.
[5] N.A. Amos *et al.* Nucl. Phys. B 262 (1985) 689.
[6] N.A. Amos *et. al.* Phys. Rev. Lett. 63 (1989) 2784.
[7] N.A. Amos *et. al.* Phys. Lett. B 247 (1990) 127, and references therein.
[8] N.A. Amos *et. al.* Phys. Rev. Lett. 68 (1992) 2433.
[9] M. M. Block and R.N. Cahn, Phys. Lett. B 188 (1987) 143.
[10] A.S. Carroll *et al.* Phys. Lett. B 80 (1979) 423.
[11] D. Bernard *et al.* Phys. Lett. B 198 (1987) 583.
[12] G. Arnison *et al.* Phys. Lett. B 128 (1983) 336.
[13] G. J. Alner *et al.* Z. Phys. C 32 (1986) 153.
[14] N.A. Amos *et. al.* Phys. Lett. B 243 (1990) 158.

Figure Captions.

Fig. 1 : Schematic layout of the apparatus.

Fig. 2 : a) Scatter plots for conjugate pots for one run before background subtraction. The elastic events lie on the diagonal; b) Scatter plot for non-conjugate pots.

Fig. 3 : The measured y-dependence for $p\overline{p}$ elastic scattering at $\sqrt{s} = 1020\ GeV$ after background subtraction. The solid line is the fit to an exponential function in y^2 in the range $161.3 \leq y^2 \leq 501.8\ mm^2$.

Fig. 4 : Energy dependence of the logarithmic slope parameter b for the $p\overline{p}$ elastic scattering distribution (data from this experiment and from references [1−8]).

Fig. 5 : Compilation of proton-antiproton σ_{tot} plotted versus s (data from this experiment and from references [8,10−14]). The dashed curve shows the behaviour of the proton-proton cross section.

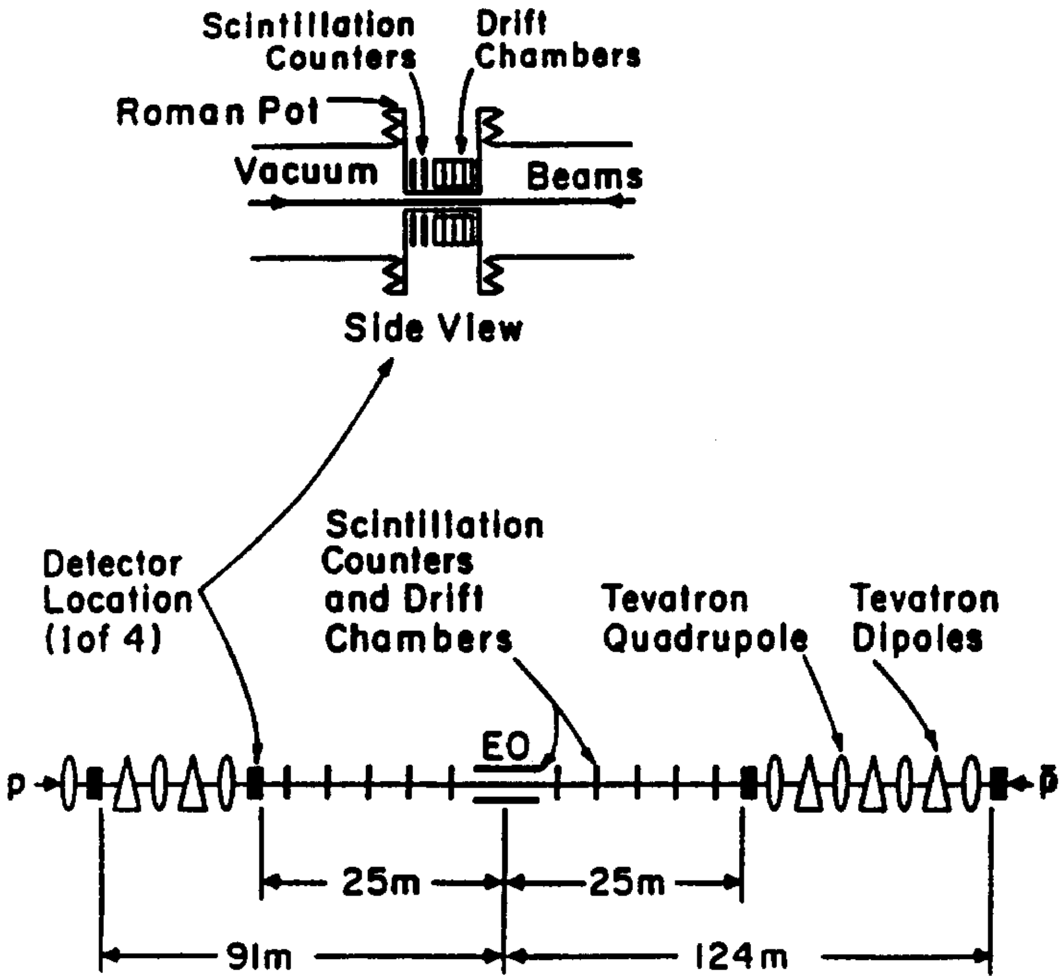

Scintillation Counters
Drift Chambers
Roman Pot
Vacuum
Beams
Side View
Detector Location (1of 4)
Scintillation Counters and Drift Chambers
Tevatron Quadrupole
Tevatron Dipoles
EO
p
p̄
25m
25m
91m
124m

Figure 1

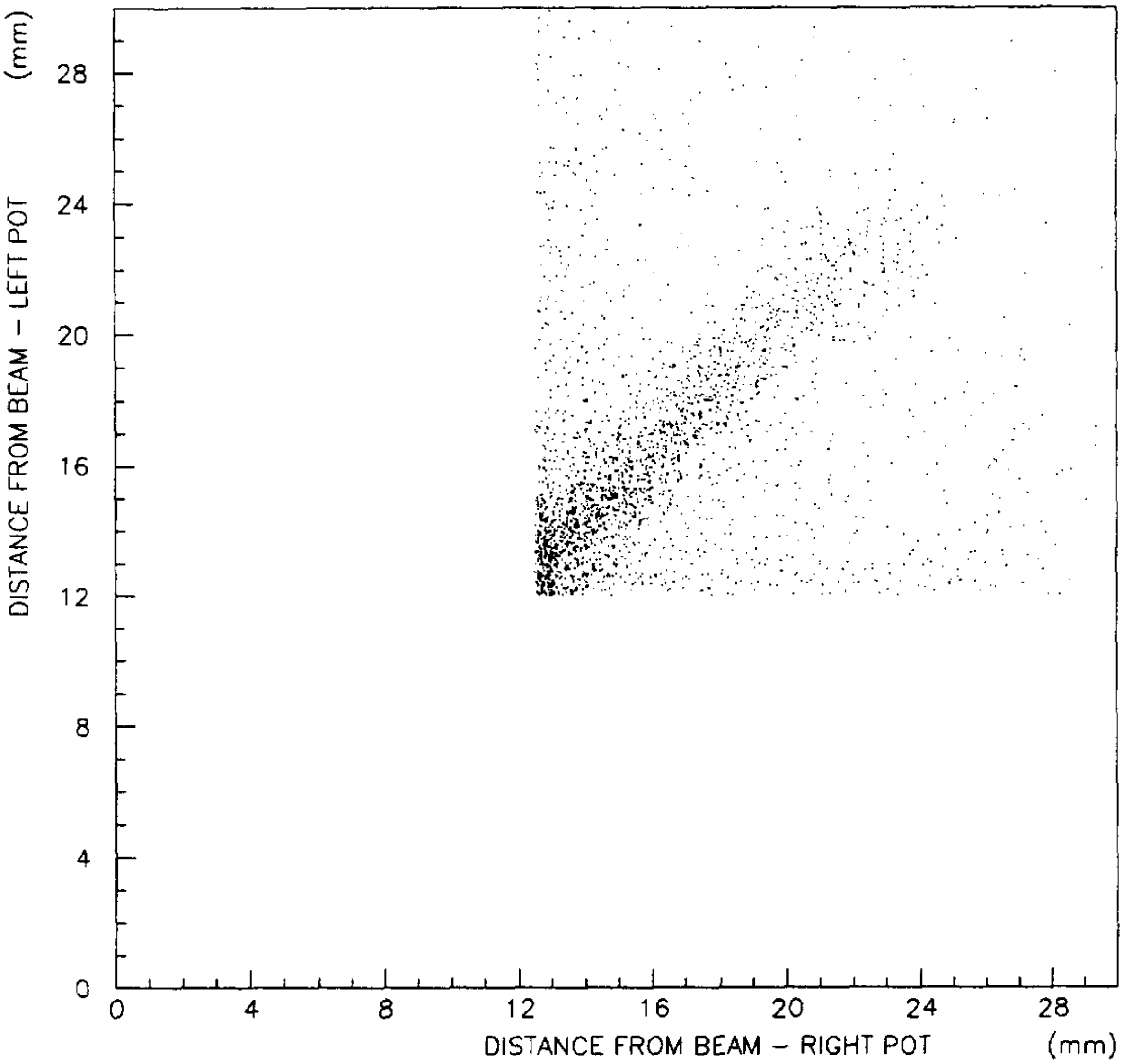
DISTANCE FROM BEAM – LEFT POT (mm)
DISTANCE FROM BEAM – RIGHT POT (mm)
0
4
8
12
16
20
24
28

Figure 2 a)

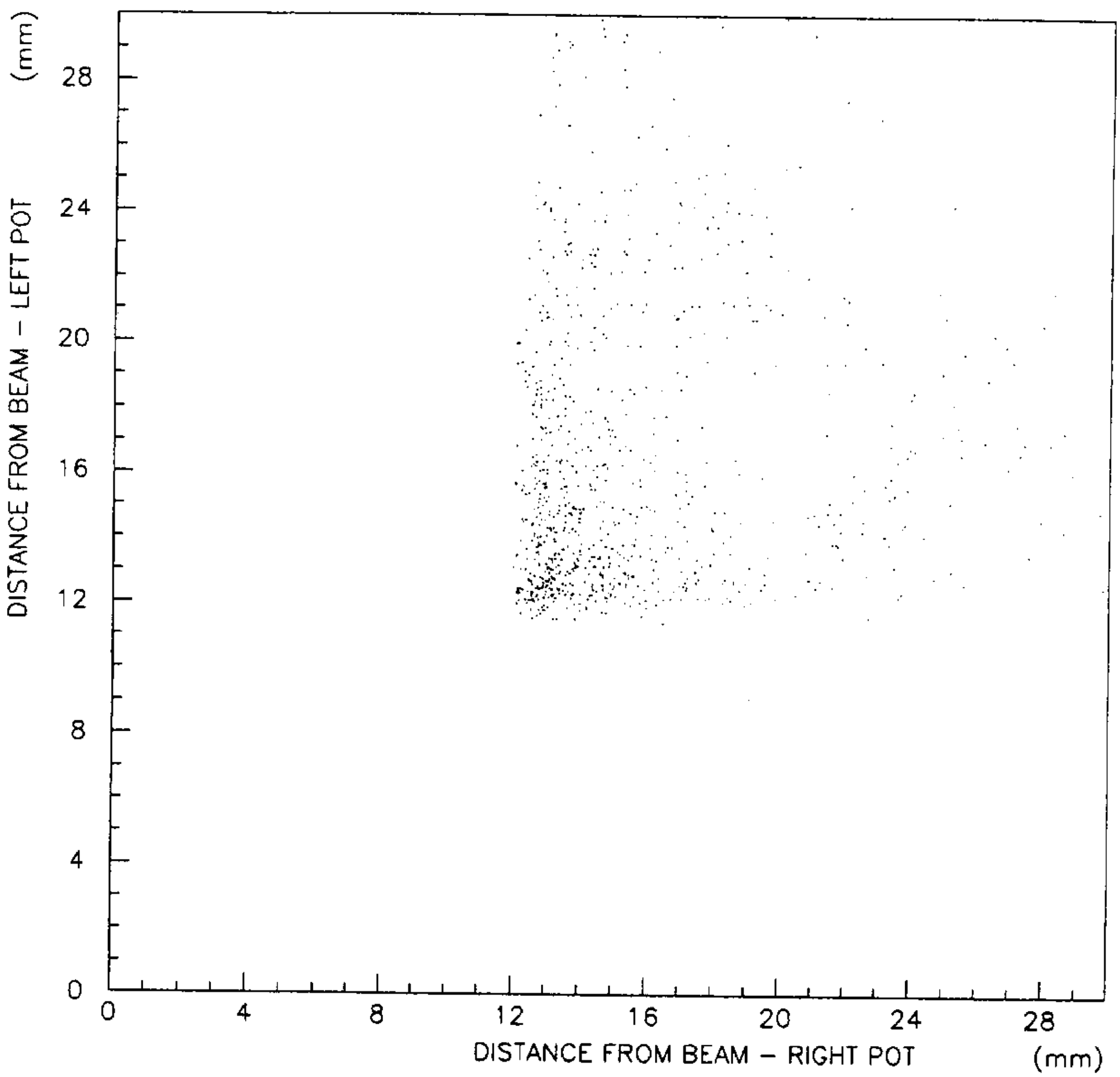

DISTANCE FROM BEAM – LEFT POT (mm)
0
4
8
12
16
20
24
28
0 4 8 12 16 20 24 28
DISTANCE FROM BEAM – RIGHT POT (mm)

Figure 2 b)

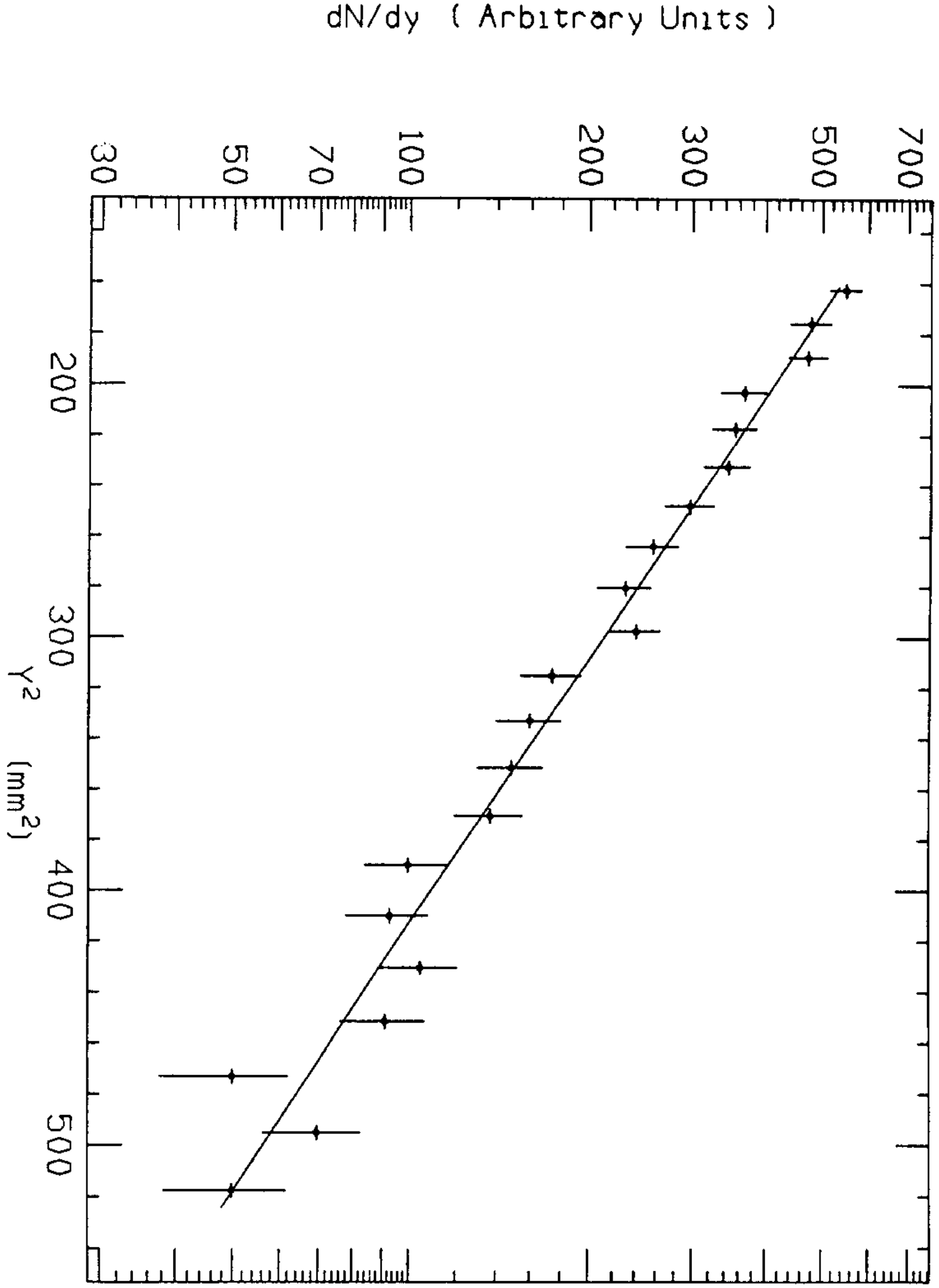
dN/dy (Arbitrary Units)
30
50
70
100
200
300
500
700
200
300
400
500
Y2 (mm2)

Figure 3

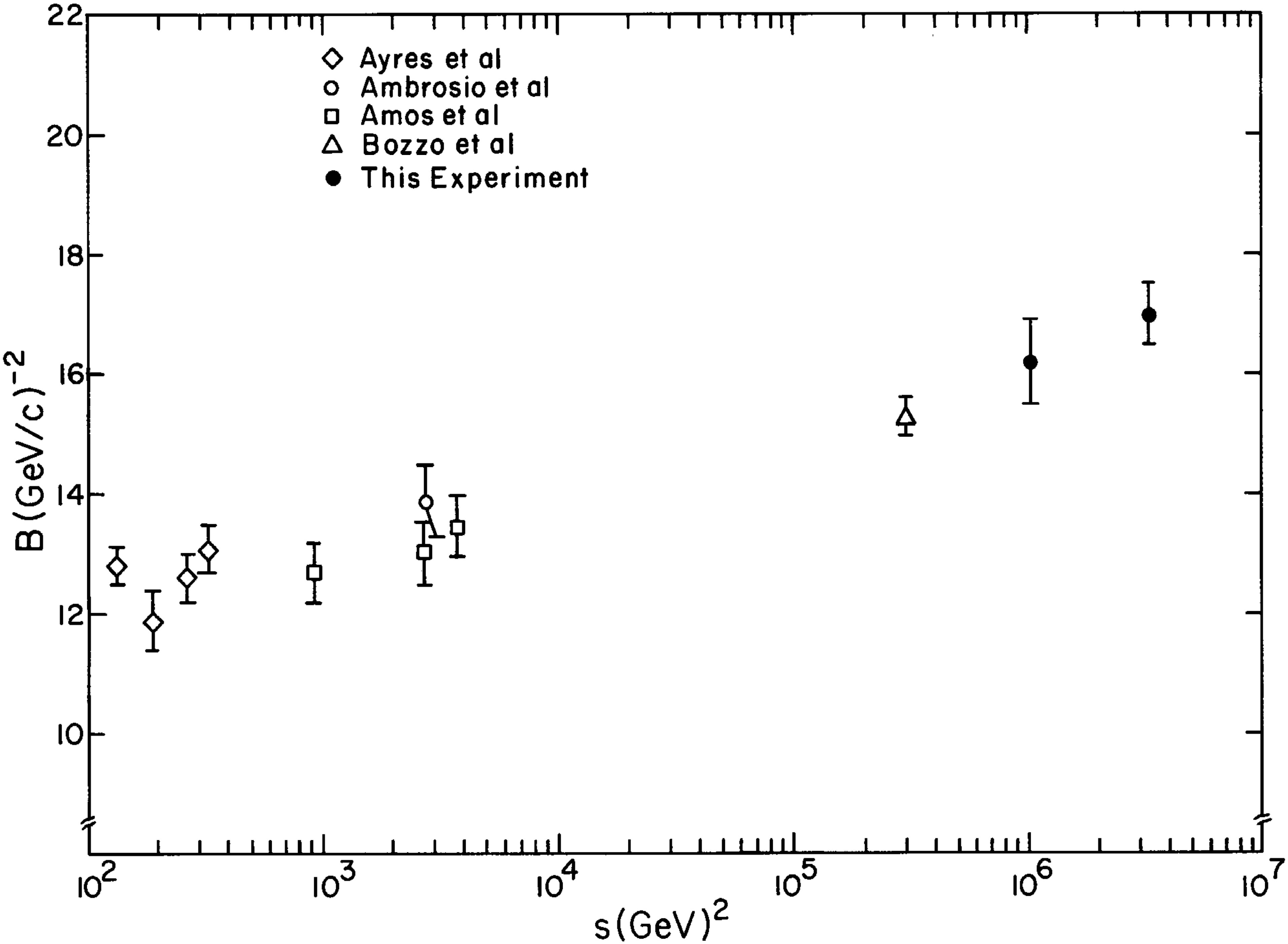

Ayres et al
Ambrosio et al
Amos et al
Bozzo et al
This Experiment
22
20
18
16
14
12
10
B(GeV/c)^-2
10^2
10^3
10^4
10^5
10^6
10^7
s(GeV)^2

Figure 4

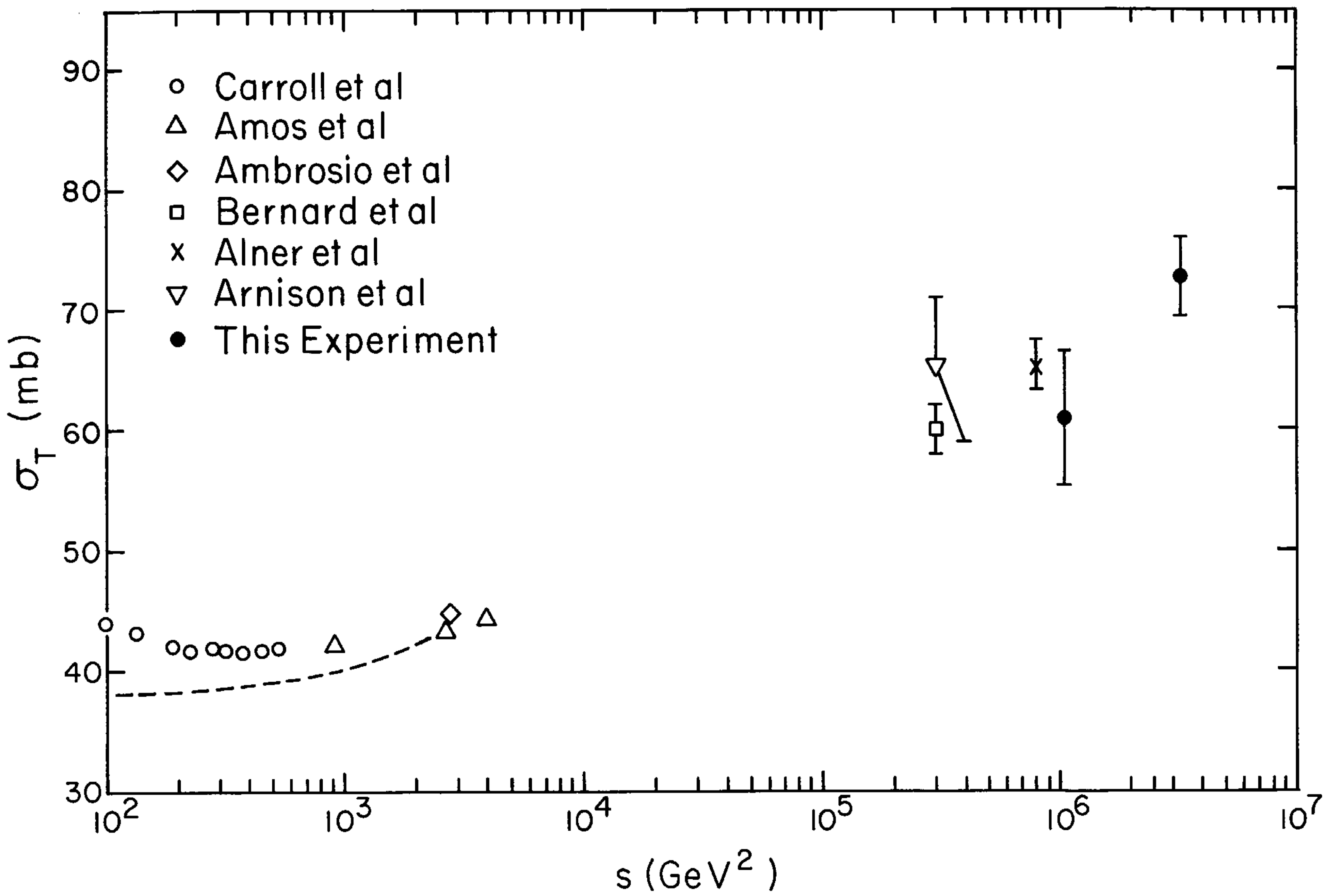

Carroll et al
Amos et al
Ambrosio et al
Bernard et al
Alner et al
Arnison et al
This Experiment
σT (mb)
90
80
70
60
50
40
30
10^2
10^3
10^4
10^5
10^6
10^7
s (GeV^2)

Figure 5